Nanoscale

Accepted Manuscript

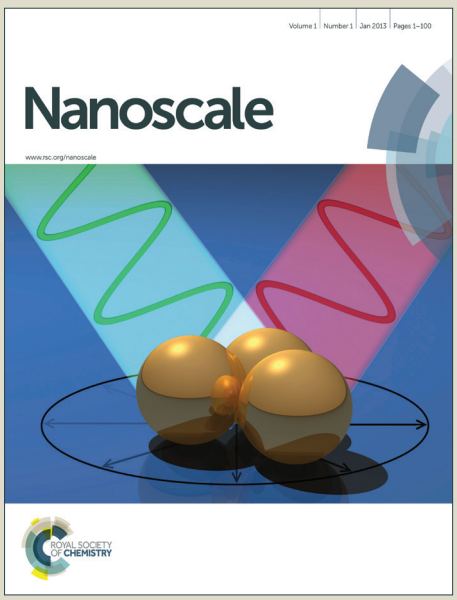

ROYAL SOCIETY OF CHEMISTRY

www.rsc.org/nanoscale

Metabolomic profiles delineate potential role of glycine in gold nanorod-induced disruption of mitochondria and blood-testis barrier factors in TM-4 cells

Bo Xu[a, b,1], Minjian Chen[a, b,1] , Xiaoli Ji[a, b,1], Zhilei Mao[a, b], Xuemei Zhang[a, b], Xinru Wang [a, b], Yankai Xia [a, b, *]

[a]State Key Laboratory of Reproductive Medicine, Institute of Toxicology, Nanjing Medical University, Nanjing 211166, China

[b] Key Laboratory of Modern Toxicology of Ministry of Education, School of Public Health, Nanjing Medical University, Nanjing211166, China

[1] The authors contributed equally.

[*] **To whom correspondence should be addressed:**

Yankai Xia, Ph.D.

State Key Laboratory of Reproductive Medicine, Institute of Toxicology,

Nanjing Medical University, 818 East Tianyuan Road, Nanjing 211166, China.

Tel: +86-25-86868425 Fax: +86-25-86868427

E-mail: yankaixia@njmu.edu.cn

Abstract

Gold nanorods (GNRs) are commonly used nanomaterials with potential harmful effects on male reproduction. However, the mechanism by which GNRs affect male reproduction remains largely undetermined. In this study, the metabolic changes in Spermatocyte-derived cells GC-2 and Sertoli cell line TM-4 were analyzed after GNRs treatment for 24h. Metabolomic analysis revealed that glycine was highly

decreased in TM-4 cells after GNRs-10nM treatment while there was no significant change in GC-2 cells. RT-PCR showed that the mRNA levels of glycine synthases in mitochondrial pathway were decreased after GNRs treatment, while there were no significant difference for mRNA levels of glycine synthases in cytoplasmic pathway. High content screening (HCS) showed that GNRs decreased membrane permeability and mitochondria membrane potential of TM-4 cells, which was also confirmed by JC-1 staining. In addition, RT-PCR and Western blot indicated that the mRNA and protein levels of blood-testis barrier (BTB) factors (ZO-1, occludin, claudin-5, connexin-43) in TM-4 cells were also disrupted by GNRs. After the replenishment of glycine, the GNRs-induced harmful effects on mitochondria and BTB factors were recovered in TM-4 cells. Our results firstly showed that even low doses of GNRs could induce significant toxic effects on mitochondria and BTB factors in TM-4 cells. Furthermore, we revealed that glycine was a potentially important metabolic intermediary for the changes of membrane permeability, mitochondria membrane potential and BTB factors after GNRs treatment in TM-4 cells.

Keywords Sertoli cells; Gold nanorods; Metabolic analysis; glycine; Mitochondria;

Abbreviations

MTT, 3-(4,5)-dimethylthiahiazo(-z-y1)-3,5-*di*-phenytetrazoliumromide;

GNRs, Gold nanorods; HCS, High content screening; GC-2, Spermatocyte-derived cells; TM-4, Sertoli cell line; BTB, blood-testis barrier; TEM, Transmission electronmicroscopy.

1.Introduction

During the past decade or so, nanorods have opened up even more possibilities for sensing and imaging applications[1]. Gold nanorods (GNRs) have been the focus of research and have attracted practical attention for biomedical applications, such as cancer diagnostics, treatment, imaging[2], drug delivery[3], food industry (food packaging, beverages) and environment remediation. Although gold nanoparticles were thought to be ‘‘nontoxic’’[4-8], recent experiments *in vivo* and *in vitro* have confirmed that GNRs could cause health problems. It has been reported that GNRs can induce cellular toxicity[9, 10] and hepatotoxicity in mouse[11, 12]. As GNRs can cross the blood-testis barrier (BTB) and deposit in the testes[13], their effects on male reproduction are the major concern. Indeed, spermatotoxicity of GNRs was reported in human[14]. However, the mechanism by which GNRs affect male reproduction remains largely undetermined. Sertoli cells provide structural and nutritional support to germ cells during spermatogenesis, and are the main components of the BTB whose connections are gap junction and tight junction. GC-2 cell line was originally derived from immortalized mouse spermatogonia, and TM-4 cell line was derived from mouse Sertoli cells. Therefore, these two cell lines (GC-2 and TM-4) provide a useful model in testing the GNRs-induced male reproductive toxicity and underlying mechanism.

The high-throughput omics analysis includes transcriptomics, proteomics, metabolomics and so on. Transcriptomics and proteomics analysis have been widely used. Currently, metabolomics is a recently-developed approach in detecting dynamic variations in small molecules and assessing functional changes in different

biochemical pathways due to chemicals exposure and diseases. Therefore, it is commonly applied in understanding multiple physiological processes. Multiple studies have shown that metabolomics delivers sensitive and quantitative biomarkers in diagnosis and treatment of diseases[15, 16], while also elucidates biological mechanisms[17] and predicts the toxicity of chemicals[18].

In this study, to better understand the toxic effects of GNRs on male reproduction and the molecular mechanisms, we applied a hypothesis-free metabolomic analysis to study GNRs-induced metabolic changes in GC-2 and TM-4 cells. According to metabolomic results, additional experiments were conducted to explore the underlying mechanism related to the observed metabolic alteration.

2. Experimental

Chemicals and reagents

GNRs (product number:716812) with dimensions of (9–11)nm×(34–42)nm were purchased from Sigma-Aldrich (St. Louis, MO, USA). GNRs were well dispersed in the medium and no aggregation was found (Figure 1A). Dimethyl sulfoxide (DMSO), glycine, bovine serum albumin (BSA), diethylpyrocarbonate (DEPC), 3-(4, 5-dimethylthiazol-2-yl)-2, 5-diphenyl tetrazolium bromide (MTT) were obtained from Sigma-Aldrich (St. Louis, MO, USA). GNRs were stored at 4 °C， and then diluted to desired concentrations in culture medium immediately before use. All chemicals were of analytical grade. DMEM medium, fetal bovine serum (FBS), streptomycin sulfate, penicillin G sodium and phosphate-buffered saline with Ca^{2+} and Mg^{2+} (PBS) were obtained from Gibco BRL (Grand Island, NY, USA). Cellular ATP levels were

measured using a firefly luciferase ATP assay kit (Beyotime, China). ROS content was detected by Reactive Oxygen Species Assay Kit (Beyotime, China). JC-1was detected by Mitochondrial Membrane Potential Assay Kit (Beyotime, China).

Cell culture and GNRs treatment

GC-2 spd(ts) (ATCC # CRL-2196) and TM-4 (ATCC # CRL -1715) cells were purchased from ATCC (Manassas, VA, USA) and cultured in complete growth medium DMEM, supplemented with 10% FBS, 100 U/mL penicillin, and 100 μg/mL streptomycin at 37°C, 5% CO_2. The final concentrations of GNRs were 0.1, 1, 10 nM. Then, the freshly diluted nanorods of different concentrations were administered when the cell confluency reached up to 50%, and the cells were treated for 24 h.

The characteristics of GNRs

Transmission electronmicroscopy (TEM) images were recorded using a Jeol JEM-2011 TEM equipped with a Gatan Dual Vision 600 CCD.

Cell viability assay

Cellular viability was evaluated by the MTT proliferation assay. MTT (5 mg/ml) was dissolved in PBS, sterilized by filtration through a 0.22 μm Millipore® filter and stored at 4 °C. Cells were plated at a density of 1.5×10^4 per well in 96-well plate and incubated overnight. After exposure to GNRs at different concentrations, the cells were washed twice with PBS. Then 25μl of MTT were added to each well, and the cells were incubated for 4h at 37°C to allow MTT metabolism. The medium was replaced with 150μl DMSO, plates were shaken for 10 min, and the absorbance was determined at 490 nm.

Cell cycle analysis and apoptosis assay

To determine if GNRs could affect the cell cycle and induce apoptosis, flow cytometric analysis was used to determine the state of cell cycle and apoptosis. Cells were seeded at a density of about 1×10^6 cells per well. Cells were incubated overnight and subsequently exposed to GNRs-10 nM or control medium. After 24h, cells were washed with PBS and harvested with trypsin/EDTA. Cells were fixed in 75% ethanol for 2h or washed in cold PBS, then stained with propidium iodide (PI) and annexin V for 30 min protected from light. The fixed/stained cells were analyzed by FACS Calibur Flow Cytometry (BD Biosciences, NJ, USA) to quantify cell cycle or cell apoptosis.

Metabolomic analysis

The metabolomic analysis of cells was basically according to previous reports[19]. GC-2 and TM-4 cells with 80% confluency in a 10 cm dish were exposed to GNRs (0, 10 nM) for 24 h. The medium was removed followed by washing the cells five times with ice cold PBS. After 1mL 50% methanol was added, the cells were harvested by scraping. Then the cells were ultra-sonicated 5 min (power: 60%, pulses: 6/4), and the supernatant was obtained after centrifuged at 12000rpm for 15min. Metabolite extraction was subsequently carried out to isolate metabolites from the freeze-dried supernatant. 500μl L-2-Chlorophenylalanine was added to the prepared cell samples and vortexed for 10 s, followed by centrifugation (12000rpm,10 min) at 4°C. 350μl supernatant was transferred into 2ml vial, and then samples were blow-dried by moderate nitrogen, this step was repeated until all of the supernatant was transferred

and dried in the vial. 80μl methoxyamine was then added, mixed moderately and reacted for 2h at 37°C. Finally, 100μl BSTFA reagent (containing 1% TMCS) was added into the mixture, reacted for 60 min at 70°C. After the above reactions, samples were cooled to room temperature and then analyzed. GC/TOFMS analysis was performed using an Agilent 7890 gas chromatography system coupled with a Pegasus 4D time-of-flight mass spectrometer. The system utilized a DB-5MS capillary column coated with 5% diphenyl cross-linked with 95% dimethylpolysiloxane (30 m×250 μ m inner diameter, 0.25 μ m film thickness; J&W Scientific, Folsom, CA, USA). A 1 μ L aliquot of the sample was injected in splitless mode. Helium was used as the carrier gas; the front inlet purge flow was 3 mL/ min; the gas flow rate was 1 mL/ min. The initial temperature was kept at 80 °C for 0.2min, then raised to 180 °C at a rate of 10 °C/ min, then to 240 °C at a rate of 5 °C /min and finally to 290 °C at a rate of 20 °C/ min. The injection, transfer line and ion source temperatures were 280, 270, and 220 °C respectively. The energy was -70 eV in electron impact mode. The mass spectrometry data were acquired in full-scan mode with the m/z range of 20–600 at a rate of 100 spectra per second after a solvent delay of 492 s.

RNA isolation and quantitative Real-time PCR assay

Total RNA was isolated using TRIZOL reagent (Invitrogen, Carlsbad, CA) according to the manufacturer's instructions, and the concentration of total RNA was determined by measuring the absorbance at 260 nm by NanoDrop 2000 (Thermo Fisher Scientific, Wilmington, DE). cDNA synthesis for coding genes were performed with 1 μg of total RNA according to the manufacturer's instructions (Takara, Tokyo, Japan).

The mRNA levels of glycine synthesizing enzyme genes (SHMT2, MTHFD1L, SHMT1, MTHFD1)

The mRNA levels of glycine synthesis (SHMT2, MTHFD1L, SHMT1, MTHFD1) were analyzed using SYBR PCR Master Mix reagent kits (Takara) according to the manufacturer's instructions. Primer sequences are shown in Table S1. All oligonucleotide primers were synthesized by Invitrogen (Shanghai). All real-time PCR reactions were carried out on ABI7900 Fast Real-Time System (Applied Bio systems, Foster City, CA, USA) according to the manufacturer's instructions. All experiments were repeated at least three times.

The expression levels of junction factors (Claudin5, Occludin, ZO-1, Connexin-43, GAPDH)

The expressions of mRNA (Claudin5, Occludin, ZO-1, Connexin-43, GAPDH) were analyzed using SYBR PCR Master Mix reagent kits (Takara) and carried out on ABI7900 Fast Real-Time System (Applied Bio systems, Foster City, CA, USA) according to the manufacturer's instructions. Primer sequences are shown in Table S1. The protein levels of these factors were detected by Western blot as previous study[20]. Antibodies for Claudin5 (23 kDa), Occludin (59 kDa), ZO-1 (220 kDa), Connexin-43 (43 kDa) and GAPDH (34 kDa) were bought from Abcam (Kendall square, MA, USA, 1:1000 dilution). All experiments were repeated at least three times.

Multiparametric assay using high content screening assay

Cell-based high-content screening (HCS) multi-parameter cytotoxicity analysis [Thermo Scientific Cellomics ®ArrayScan ® V^{TI} HCS Reader (Pittsburgh, USA)] was

used to measure GC-2 and TM-4 cells health status after GNRs exposure. GC-2 and TM-4 cells were plated at a density of $5*10^4$cells/ml in Collagen I-coated 96-well plates (BD Biocoat® Plates, No. 354407) and incubated for 24 h. After exposure to GNRs-10 nM, GNR-10 nM +5mM Glycine, control medium or positive control (120 μM Valinomycin) for 24 h, cells were fixed and stained for imaging analysis using Cellomics® Multiparameter Cytotoxicity 3 Kit (8408102; Cellomics) according to the manufacturer's instructions. Cell images and data were automatically obtained from HCS. Appropriate filter sets for detection of four fluorophores were used, and different fluorescent signals were recorded in four different image collection channels. Channel 1 contained the blue nucleus images stained with Hoechst 33342; Channel 2 contained the green cell membrane stained with green permeability dye; Channel 3 contained the yellow mouse monoclonal antibody against cytochrome c. Channel 4 contained the red mitochondria mass images stained with mitochondria membrane potential Dye. For each cell treatment, four independent wells were measured. The 20× objective was used to collect images for the distinct fluorescence channels. To capture enough cells (>500) for the analysis, 16 fields per well were imaged. The analysis was performed by using the Automated Image and Data Analysis Software.

Analysis of the Reactive oxygen species (ROS) content

To determine if GNRs could affect the content of intracellular ROS, flow cytometric analysis was used to detect the oxidation-sensitive probe DCFH-DA. TM-4 Cells were incubated overnight and subsequently exposed to GNRs-10 nM, GNRs-10nM +Gly-5mM or control medium. After 24h, cells were washed with PBS and harvested

with trypsin/EDTA. The cellular fluorescence intensity was measured after 30 min incubation with 5 μM DCFH-DA at 37 ℃, followed by FACS Calibur Flow Cytometry (BD Biosciences, NJ, USA).

Detection of the Cellular ATP levels

Cellular ATP levels were measured using a firefly luciferase ATP assay kit (Beyotime, China) according to the manufacturer's instructions. After being cultured in GNR-10 nM, GNRs-10nM +Gly-5mM or control medium, 200 μ L lysis buffer from the ATP detection kit was added into a well of 6-well plates. Each cell culture was collected and centrifuged at 12,000 rmp for 5 min at 4℃. The supernatant was transferred to a new tube for ATP test. The luminescence from a 100 μ L sample was assayed in a 96-well plate luminometer (Berthold Detection System, Pforzheim, Germany) together with 100 μ L ATP detection buffer from the ATP detection kit. The standard curve of ATP concentration was prepared from a know amount (0-10 μ M).

Mitochondria membrane potential assay by JC-1

Cells were seeded at a density of about 1×10^6 cells per well. Cells were incubated overnight and subsequently exposed to GNRs-10 nM, GNRs-10 nM+Gly-5mM, or control medium for 24h. The positive control (10 μ M CCCP) was incubated for 20 minutes. The cells were washed with PBS and harvested with trypsin/EDTA, then incubated with 2 ml of medium containing JC-1 staining probe for 20 min at 37° C and washed twice with staining buffer. Some cells were resuspended in 1 ml of PBS and analyzed by a Flow Cytometry to detect green and red fluorescence. The other JC-1-stained cells were measured by confocal fluorescence microscopy. The

wavelengths of excitation and emission were 514 nm and 529 nm for detection of monomer form of JC-1, and 585 nm and 590 nm were used to detect aggregate of JC-1.

Data analysis

Values are expressed as means ± standard error of the mean (S.E.) for all experiments. Statistically significant differences between the treatments and the control were determined by one-way ANOVA, followed by Dunnett's multiple comparison test. We used the method of $2^{-\Delta\Delta Ct}$ to analyze the results of RT-PCR in all of our experiments. Statistical analysis was performed using STATA9.2 and presented with GraphPAD prism software. All tests of statistical significance were two-sided, and the statistical significance was set at $p < 0.05$. Significant differences of metabolites between treatment group and control group were tested using T-test analysis. Bonferroni correction and FDR (False discovery rate) correction were used to counteract the problem of multiple comparisons.

3. Results and discussion

Effects of GNRs on cell viability

To identify the effects of GNRs on cell viability, GC-2 and TM-4 cells were exposed to various concentrations of GNRs for 24h and 48h. As shown in Figure 1B and 1C. GNRs treatment didn't affect cell viability at 10nM while GNRs with higher dose caused decreased cell viability. Since neither exposure to GNRs-10nM for 24h nor 48h induced cytotoxic effects, in all of the following experiments, cells were exposed to GNRs for 24h. Although there was no cytotoxicity in GC-2 and TM-4 cells after

GNRs-10nM exposure, previous reports showed that nanoparticles were associated with reproductive toxicity, therefore, the patterns may vary for different nanoparticle preparations[21].

Effects of GNRs on cell cycle and apoptosis

We examined the effects of GNRs on the cell cycle and apoptosis after 24h exposure by flow cytometery. We found no significant differences in cell cycle and apoptosis between treated and the control group both in GC-2 and TM-4 cells (Figure 1D and 1E).

Metabolic changes with GNRs exposure

The total ion chromatogram (TIC) of 12 samples identified 412 kinds of metabolites. There was no overall chromatographic difference between sample groups, and the retention time was reproducible and stable, indicating the reliability of metabolomic analysis. According to PCA analysis, obvious separations between samples in both treatment and control groups were detected in TM-4 (Figure 2A) and GC-2 cells (Figure S1). To identify robust and key metabolism alteration, the statistical analyses include the comparison of metabolite level between control and treatment group as well as metabolic pathway enrichment analysis using MetaboAnalyst. After FDR correction, 8 metabolic pathways were significantly changed, among which the p value of Glycine, Serine and Threonine metabolism was the lowest in TM-4 cells (Figure 2B). We found 47 up-regulated small molecules and 42 down-regulated small molecules ($p<0.05$). After strict Bonferrion correction (p cutoff <0.0001) was applied, 9 statistically robust alterations of metabolites were identified (4 up-regulated

metabolites and 5 down-regulated metabolites) (Figure 2C). Interestingly, glycine was among the down-regulated small molecules after Bonferrion correction, while it is also the core metabolite in Glycine, Serine and Threonine metabolism pathway. Therefore, glycine was the most robust altered metabolite in TM-4 cells according to the metabolomic analysis. However, when above analyses were conducted using data obtained from GC-2 cells, no positive results were observed (Figure S1). Thus, we then focused on the glycine changes to study the underlying mechanism of GNRs on TM-4 cells.

The mRNA levels of glycine synthesizing enzyme genes

Glycine is a non-essential amino acid that can be endogenously synthesized. Intracellular glycine synthesis occurs in the cytosol and mitochondria with two separate enzymatic pathways[22]. The glycine synthesizing enzymes SHMT2 and MTHFD1L are responsible for mitochondria glycine synthesis while SHMT1 and MTHFD1 are responsible for the cytosol glycine synthesis. The decreased glycine maybe related with these intracellular glycine synthase. Our results showed that the glycine synthases in mitochondrial pathway were decreased after GNRs treatment, while there was no significant difference for the glycine synthases in cytoplasmic pathway (Figure 3A).

The mRNA and protein levels of BTB factors

As Sertoli cells are the main components of the BTB, whose connections are gap junction and tight junction, we detected the effects of GNRs on BTB by examining the mRNA and protein levels of gap junction factor (connexin-43) and tight junction

factors (ZO-1, claudin-5, occludin). Exposure to GNRs-10nM in TM-4 cells significantly increased the mRNA and protein levels of connexin-43, ZO-1, claudin-5, and occludin. To explore whether glycine plays any roles in these disruptions, glycine was added to see if these changes reversed. Interestingly, after supplementation of 5mM glycine, the mRNA and protein levels of BTB factors were recovered (Figure 3B, 3C).

Dysfunction of the BTB factors is an important mechanism involved in chemical-induced reproductive toxicity[23]. The BTB between Sertoli cells is created by the coexistence of several proteins, including tight junction, gap junction, desmosome-like, and basal ectoplasmic specialization proteins[24]. Junctions factors in Sertoli cells have been considered as early targets for reproductive toxicants and might contribute to the toxic effects on reproduction system[25]. Previous studies reported pulsatile shear stress, Hypoxic stress, MG-132, T (testosterone), DHT and androgens affected spermatogenesis via increasing the junction factors and regulation of the BTB[26-29], suggesting that the increased expressions of junctions factors might disrupt the junction assembly. Therefore, increases in tight junction factors (claudin-5, occludin, ZO-1) and gap junction factor (connexin-43) mRNA expressions might be important molecular mechanisms for GNRs- induced disruption of the BTB between Sertoli cells, and glycine plays an important role in these disruptions.

HCS multi-parameter cytotoxicity analysis of GNRs

HCS multi-parameter cytotoxicity analysis showed that GNRs-10 nM had no cytotoxicity to GC-2 cells after incubation for 24 h compared with control (Figure S2).

However, TM-4 cells exposed to GNRs showed lower cell permeabilization ($P<0.05$) and decreased mitochondria membrane potential ($P< 0.05$), whereas no changes were observed in the nuclear size and cytochrome c. Figure 4 showed that the cell membrane permeability dye stained weakly in green fluorescence, and mitochondria membrane potential dye stained weakly in red fluorescence when treated with GNRs. These changes were rescued by the addition of glycine to the medium after GNRs exposure, indicating glycine plays an important role in these disruptions caused by GNRs. Valinomycin is a classical K^+ ionophore, and is well known to disturb the mitochondrial function[30]. In this study, we used Valinomycin as the positive control compound. Treatment with Valinomycin resulted in cell loss, nuclear condensation, changed cell permeability, loss of mitochondrial membrane potential and cytochrome c release (Figure S2, Figure 4).

There are several reports indicating nanoparticles could induce remarkable loss of mitochondria membrane potential[31-33]. We found decreased mitochondria membrane potential ($P< 0.05$) and decreased glycine when TM-4 cells were exposure to GNRs and such changes could be rescued by glycine supplement, indicating the GNRs-induced mitochondria damage and glycine played an important role in these changes caused by GNRs.

Glycine involved in the body's production of phospholipids. Phospholipids are the major component of cell membranes. Nanoparticles with different shapes and sizes would impact the cell membrane permeability differently[34]. Our results showed that GNRs-induced low cell permeabilization ($P<0.05$) which can be recovered by

glycine supplement. Therefore, our data indicated that glycine plays an important role in cell permeabilization changes caused by GNRs.

Effects of GNRs on cellular ATP levels and ROS content

We examined the effects of GNRs on ATP levels/ROS content after 24h exposure by luminometer/flow cytometery. We found no significant differences in ATP levels/ROS content between the treated groups and the control in TM-4 cells (Figure 5A-D).

Mitochondria membrane potential assay by JC-1

To further determine the effects of GNRs on mitochondrial membrane potential, we used another classical JC-1 staining detection by Flow Cytometry and Confocal fluorescence microscopy. Flow Cytometry results showed that the ratio of aggregate/monomer in GNRs-10 nM group was slightly lower than the control. After the replenishment of glycine, the GNRs–induced decrease was recovered (Figure 5E, 5F). There were consistent results showed by confocal fluorescence microscopy (Figure 5G). Overall, the JC-1 staining results indicated that GNRs-10nM could induce decreased mitochondria membrane potential, which is consistent with our HCS results.

Although the loss in mitochondrial membrane potential is often associated with changes in ATP levels, ROS content and cell apoptosis, these changes do not always appear simultaneously. Our results indicated that GNRs-10nM induced the loss of mitochondrial membrane potential using three different detection methods (HCS, Flow Cytometry and Confocal fluorescence microscopy), while there were no significant difference in ATP levels, ROS content and cell apoptosis. Our results are

consistent with previous studies[35, 36].

4. Conclusions

Our metabolomics data provide a novel understanding of metabolic changes in male reproductive cells exposure to GNRs. Despite the lack of obvious evidence of cytotoxicity, cell cycle, apoptosis, ATP levels, ROS content changes, we revealed that GNRs caused changes of membrane permeability, mitochondria membrane potential, and BTB factors in TM-4 cells, and GNRs-induced decrease of glycine plays an important role in these disruptions.

Conflict of interest

None declared.

Acknowledgments

This study was supported by National 973 Program (2012CBA01306); National Science Fund for Outstanding Young Scholars (81322039); National Natural Science Foundation (31371524); Distinguished Young Scholars of Jiangsu Province (BK20130041); Priority Academic Program Development of Jiangsu Higher Education Institutions (PAPD)； New Century Excellent Talents in University (NCET-13-0870).

Author Contributions

Conceived and designed the experiments: YX XW BX. Performed the experiments: BX XJ MC ZM XZ. Analyzed the data: MC BX. Wrote the paper: BX.

References

1. M. CJ, G. AM, S. JW, S. PN, A. AM, G. EC and B. SC, *D - 0157313*, T - ppublish.
2. X. Huang, I. H. El-Sayed, W. Qian and M. A. El-Sayed, *J Am Chem Soc*, 2006, 128, 2115-2120.
3. P. H. Yang, X. Sun, J. F. Chiu, H. Sun and Q. Y. He, *Bioconjug Chem*, 2005, 16, 494-496.
4. A. AM, N. PK, H. CR, S. TJ, M. CJ and W. MD, *D - 101235338*, T - ppublish.
5. H. TS, G. AA and C. WC, - *Small. 2008 Jan;4(1):153-9.*, T - ppublish.
6. K. V, K. K, B. S, B. EJ, C. SW, F. GM, R. DJ, C. M, K. R and K. KV, - *Small. 2007 Feb;3(2):333-41.*, T - ppublish.
7. D. J. WH, H. WI, K. P, B. MC, S. AJ and G. RE, *D - 8100316*, T - ppublish.
8. B.-I. O, A. RM, F. VE and F. DY, - *Small. 2009 Aug 17;5(16):1897-910. doi: 10.1002/smll.200801716.*, T - ppublish.
9. P. N, F. X, S. Y, B. A, R. A, S. J, U. A and R. M, - *Small. 2006 Jun;2(6):766-73.*, T - ppublish.
10. P. Y, L. A, R. D, N. S, B. J, S. G, B. W, S. U and J.-D. W, - *Small. 2009 Sep;5(18):2067-76. doi: 10.1002/smll.200900466.*, T - ppublish.
11. J. H. Hwang, S. J. Kim, Y. H. Kim, J. R. Noh, G. T. Gang, B. H. Chung, N. W. Song and C. H. Lee, *Toxicology*, 2012, 294, 27-35.
12. W. S. Cho, M. Cho, J. Jeong, M. Choi, H. Y. Cho, B. S. Han, S. H. Kim, H. O. Kim, Y. T. Lim and B. H. Chung, *Toxicology and applied pharmacology*, 2009, 236, 16-24.
13. K. JS, Y. TJ, Y. KN, K. BG, P. SJ, K. HW, L. KH, P. SB, L. JK and C. MH, *D - 9805461*, T - ppublish.
14. V. Wiwanitkit, A. Sereemaspun and R. Rojanathanes, *Fertility and sterility*, 2009, 91, e7-8.
15. B. M, M. WR, W. L, M. T, S.-P. R, B. SS and F. B. M, *D - 0372537*, T - ppublish.
16. N. J. Serkova, Y. Zhang, J. L. Coatney, L. Hunter, M. E. Wachs, C. U. Niemann and M. S. Mandell, *Transplantation*, 2007, 83, 517-521.
17. S. M. Schieke, M. Ma, L. Cao, J. P. McCoy, Jr., C. Liu, N. F. Hensel, A. J. Barrett, M. Boehm and T. Finkel, *The Journal of biological chemistry*, 2008, 283, 28506-28512.
18. P. R. West, A. M. Weir, A. M. Smith, E. L. Donley and G. G. Cezar, *Toxicology and applied pharmacology*, 2010, 247, 18-27.
19. D. Wu, S. Cai, M. Chen, L. Ye, Z. Chen, H. Zhang, F. Dai, F. Wu and G. Zhang, *PloS one*, 2013, 8, e55431.
20. X. B, C. X, M. Z, C. M, H. X, D. G, J. X, C. C, R. VK, W. X and X. Y, *D - 101285081*, T - epublish.
21. T. Komatsu, M. Tabata, M. Kubo-Irie, T. Shimizu, K. Suzuki, Y. Nihei and K. Takeda, *Toxicology in vitro : an international journal published in association with BIBRA*, 2008, 22, 1825-1831.
22. T. AS and A. DR, *D - 8209988*, T - ppublish.
23. C. CY, W. EW, L. PP, L. MW, S. L, S. ER, Y. HH, M. J, M. PP, B. M, S. B and M. DD, *D - 101543545*, T - ppublish.
24. Q. L, Z. X, Z. Y, G. J, C. M, Z. Z, W. X and W. SL, - *Toxicol Sci. 2013 Sep;135(1):229-40. doi: 10.1093/toxsci/kft129. Epub 2013 Jun*, T - ppublish.
25. F. C, T.-E. A, C. S, C. C and P. G, *D - 8803591*, T - ppublish.

26. O. C. Colgan, G. Ferguson, N. T. Collins, R. P. Murphy, G. Meade, P. A. Cahill and P. M. Cummins, *American journal of physiology. Heart and circulatory physiology*, 2007, 292, H3190-3197.
27. B. RC, M. KS, E. RD, H. JD, B. AR and D. TP, *D - 0052457*, T - ppublish.
28. L. WY and L. WM, *D - 0050222*, T - ppublish.
29. C. NP and C. CY, *D - 0375040*, T - ppublish.
30. I. Y, Y. M, K. T, A. J, Y. T and U. K, *D - 7608465*, T - ppublish.
31. L. Qi, Z. Xu and M. Chen, *Eur J Cancer*, 2007, 43, 184-193.
32. L. Chen, R. A. Yokel, B. Hennig and M. Toborek, *Journal of neuroimmune pharmacology : the official journal of the Society on NeuroImmune Pharmacology*, 2008, 3, 286-295.
33. M. I. Khan, A. Mohammad, G. Patil, S. A. Naqvi, L. K. Chauhan and I. Ahmad, *Biomaterials*, 2012, 33, 1477-1488.
34. B. G. Trewyn, J. A. Nieweg, Y. Zhao and V. S. Y. Lin, *Chemical Engineering Journal*, 2008, 137, 23-29.
35. D. Pastore, M. Soccio, M. N. Laus and D. Trono, *BMB Reports*, 2013, 46, 391-397.
36. L. E. Klein, L. Cui, Z. Gong, K. Su and R. Muzumdar, *Biochemical and biophysical research communications*, 2013, 440, 197-203.

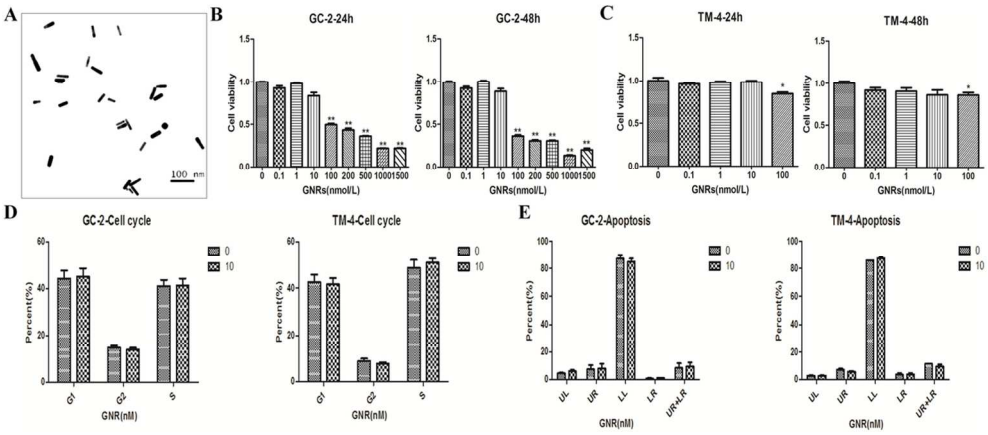

Figure 1. Effects of GNRs on cell viability in GC-2 and TM-4 cells. (A) TEM images of GNRs. (B and C) Cell viability was determined by MTT assay after exposure to various concentrations of GNRs for 24h and 48h. Values of the experiment were represented as the percentages of cell viability compared with that of the control and expressed as means ± S.E. from five separate experiments in which treatments were performed in quadruplicate. (D and E) Effects of GNRs on cell cycle and apoptosis in GC-2 and TM-4 cells. Cells were cultured with 10nM GNRs or control medium for 24 h. The cell cycle and apoptosis were analyzed by flow cytometry. 10,000 cells were analyzed for each sample. (D) The quantitated results of cell cycle in GC-2 and TM-4 cells. Data of the experiment was expressed as a percentage of total cells. (E) The percentage of apoptotic cells in GC-2 and TM-4 cells were presented in histogram. Cells in the LL quadrant indicated that they were live cells. Cells in the LR quadrant were in the early stages of apoptosis. Cells in the UR quadrant were late apoptotic. Cells in the UL quadrant indicated that they were dead cells. Each data point was represented as the means ± S.E. from three separate experiments in which treatments were performed in triplicate.

56x24mm (600 x 600 DPI)

A

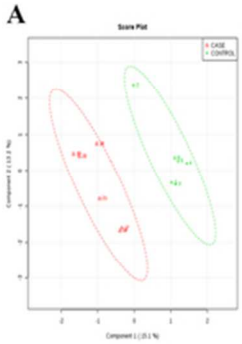

B

Metabolic pathways	Total Cmpd	Hits	Raw p	FDR	Impact
Glycine, serine and threonine metabolism	31	5	6.24E-05	0.0007281	0.35552
Cyanoamino acid metabolism	6	1	6.62E-05	0.0007281	0
Methane metabolism	9	1	6.62E-05	0.0007281	0
Porphyrin and chlorophyll metabolism	27	1	6.62E-05	0.0007281	0
Aminoacyl-tRNA biosynthesis	69	9	0.000111	0.000852	0
Primary bile acid biosynthesis	46	2	0.000116	0.000852	0.05952
Nitrogen metabolism	9	3	0.000139	0.0008763	0
Phenylalanine,tyrosine and tryptophan biosynthesis	4	1	0.0086	0.0473	0

C

Peak	KEGG	P value	P<0.05	Bonferroni correction	Fold change
fucose		9.28E-05	*	**	1.945811
L-Threose		0.000374	*	**	1.835781
Proline	C00148	0.000502	*	**	2.320738
putrescine	C02896	0.001792	*	**	1.657918

D

Peak	KEGG	P value	P<0.05	Bonferroni correction	Fold change
creatine degr	C00300	0.000273	*	**	0.291148
4-Acetamidobutyric acid		0.000452	*	**	0.178741
glycine	C00037	0.001634	*	**	0.400192
Myristic Acid	C06424	0.001669	*	**	0.836837
N-alpha-Acetyl-L-ornithine	C00437	0.00175	*	**	0.800905

Figure 2. Metabolite profiling analysis in TM-4 cells. (A) PCA plot for GC/MS data. (B) Metabolites pathways changes detected using GC/MS. (C) 4 up-regulated small molecules after Bonferroni correction. (D)5 down-regulated small molecules after Bonferroni correction.
25x8mm (600 x 600 DPI)

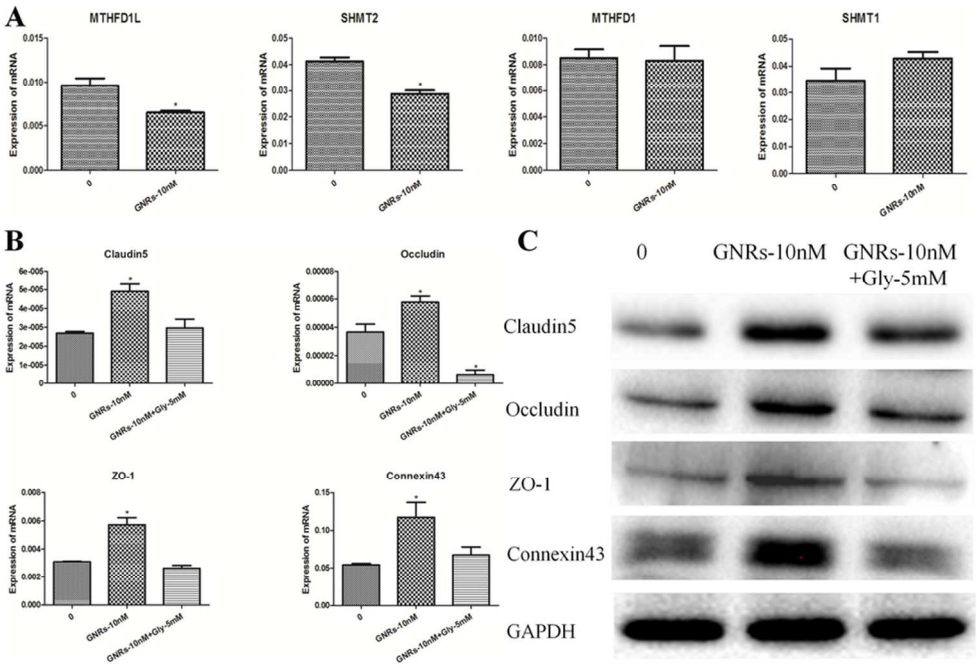

Figure 3. The expression of glycine metabolic enzymes and BTB factors in TM-4 cells. (A) The glycine synthesizing enzymes (SHMT2, MTHFD1L) in mitochondrial pathway and the glycine synthesis enzymes (SHMT1, MTHFD1) in cytosol pathway were detected by RT-PCR using a housekeeping gene GAPDH as an internal control. (B and C) The gap junction factor(connexin-43) and tight junction factors (ZO-1, claudin-5, occludin) were detected by RT-PCR and Western blot. * indicates significant difference when the values were compared to that of the control ($p < 0.05$). All tests were performed in triplicate and presented as means±SE.
42x29mm (600 x 600 DPI)

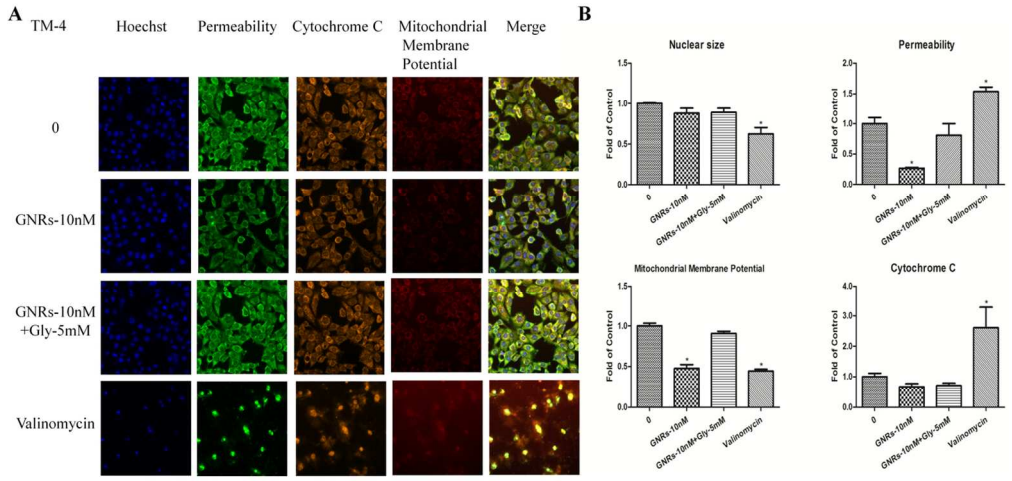

Figure 4. Representative images from the HCS after GNRs exposure to TM-4 cells. (A) Staining for nuclei (blue), cell membrane permeability (green), cytochrome c (yellow) and mitochondria membrane potential (red). Images were acquired with the ArrayScan HCS Reader with a 20 x objective. (B) The relative expressions of nuclear size, permeability, cytochrome c and mitochondria membrane potential. * indicates significant difference when the values were compared to that of the control ($p < 0.05$).
63x30mm (600 x 600 DPI)

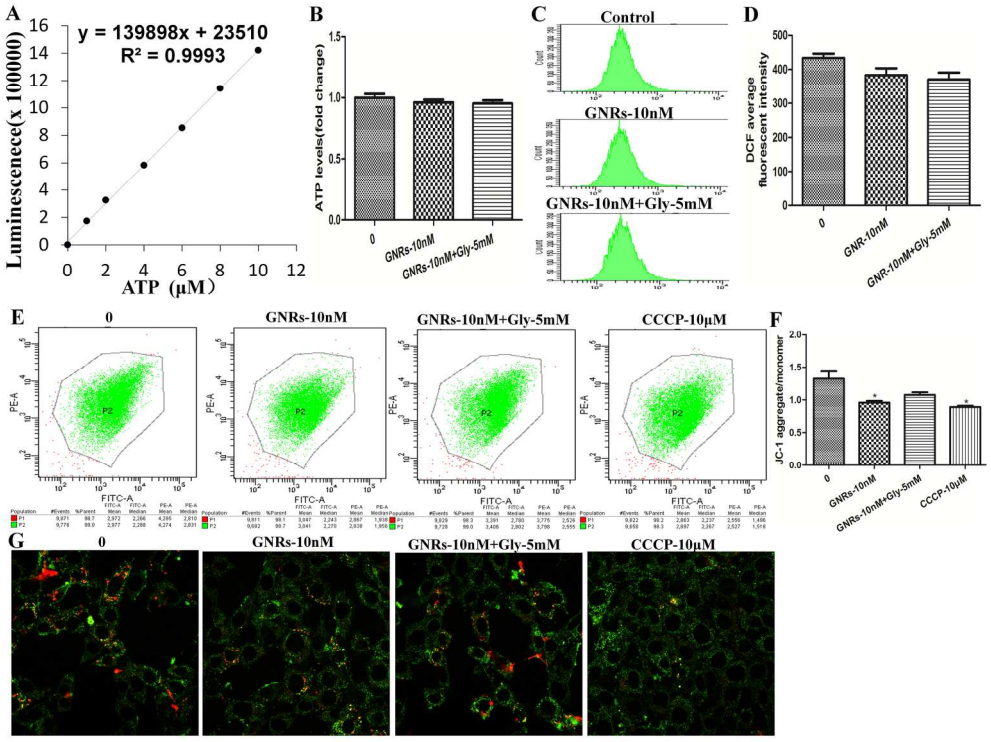

Figure 5. Comparison of ATP levels, ROS content and mitochondrial membrane potential in GNRs-10 nM, GNRs-10nM +Gly-5mM or control groups. (A) The standard curve. (B) The ATP levels of TM-4 cells after treated with GNRs-10 nM, GNRs-10nM +Gly-5mM or control medium. (C) Flow cytometry results of ROS content. x-axis, DCFH-DA fluorescence; y-axis, number of TM-4 cells. (D) The DCF average fluorescent intensity was also presented in histogram. (E) Assessment of mitochondrial membrane potential by JC-1 staining and detected by Flow cytometry. (F) The flow cytometry results of JC-1 staining was presented in histogram. (G) Assessment of mitochondrial membrane potential by JC-1 staining and detected by confocal fluorescence microscopy. Data were shown as the means ± SE. * indicates significant difference when the values were compared to that of the control ($p < 0.05$).

93x70mm (600 x 600 DPI)